Reports

Bulk Superconductivity at 122 K in $Tl(Ba,Ca)_2Ca_3Cu_4O_{10.5+\delta}$ with Four Consecutive Copper Layers

P. Haldar, K. Chen, B. Maheswaran, A. Roig-Janicki,
N. K. Jaggi, R. S. Markiewicz,* B. C. Giessen

The observed increase of superconducting transition temperature (T_c) with the number of copper oxide planes continues in the four-$[CuO_2]^{-2}$ layer (single Tl layer) oxide superconductor, which has been prepared with >80% purity and was magnetically aligned for crystallographic identification. A master scaling curve is proposed, which ties together the T_c's of virtually all known Bi and Tl oxide superconductors, and shows that the Tl(Bi) layers play an essential role in the superconductivity.

The "second-generation" superconducting cuprates containing thallium or bismuth are layered compounds with the general formula $(B^{III})_y(A^{II})_2Ca_{n-1}Cu_nO_z$, where B^{III} = Tl or Bi, A^{II} = Ba or Sr, and $z = (3/2)y + 2n + 1 + \delta$ (*1–3*). They form two homologous series with $y = 1$ and $y = 2$. It was found that within each series, the superconducting transition temperature (T_c) increases monotonically with n, the number of consecutive copper oxide layers (*4*). Phases with $y = 2$ contain Tl or Bi as double layers; ($y = 2$) compounds with n = 1, 2, and 3 have been prepared as bulk materials (*1–3*). A thallium phase of this type, $Tl_2Ba_2Ca_2Cu_3O_z$, yields the highest T_c reported to date, 125 K (*3*). Cuprates with $y = 1$ have single B^{III} oxide layers; to form these phases, B^{III} must be predominantly Tl. We have previously reported the preparation and properties of ($y = 1$) phases with $n = 1$ (1201 phase) (*5*) and $n = 2$ (1212 phase) (*6*). We have now prepared bulk samples of the single Tl layer phases with $n = 3$ [also found by Parkin *et al.*; see discussion in (*4*)] and, reported here, $n = 4$ (1234 phase); we present initial structural and superconductivity data on these phases. The ($n = 4$) phase, with four consecutive copper oxide layers (interspersed by Ca), has $T_{c(R=0)}$ = 122 K, that is, the second highest T_c reported to date [by comparison, for the ($n = 3$) phase, $T_{c(R=0)}$ = 110 K (*4*)]. This result is especially significant because it extends and quantifies the increase (*4*) of T_c with n within the ($y = 1$) series to $n = 4$. The quantitative correlation (*7, 8*) between T_c and structural data is applied to the ($y = 1$) series, extended to $n = 4$; by including a heuristic contribution from the additional B^{III} layer in the ($y = 2$) series, we can construct a master curve for both series that can be extrapolated to estimate the ultimate T_c for a "pure" cuprate superconductor.

Phases with n = 2, 3, and 4 were prepared from the mixed oxide powders, following a complex thermal treatment schedule featuring prereaction steps on heating, a high-temperature reaction step of 5 to 10 minutes at 870°C, and a normalization treatment of 10 to 12 hours at 800°C, followed by a controlled cooling/oxygenation treatment. The products were studied by x-ray powder diffraction (XRD) and four-point probe resistance and susceptibility measurements with a superconducting quantum interference device (SQUID).

In identifying the XRD patterns, we have found it useful to study also magnetically oriented samples (*9, 10*) as reported in more detail elsewhere (*11*). In such samples, the grains have a common *c*-axis direction and XRD provides definitive unit cell height information even in mixed phase samples. This is illustrated by the x-ray diffractogram, Fig. 1A, which shows the {0 0 l} lines of the phases with $n = 3$ and $n = 4$.

Depending on starting composition (which usually contained Cu oxide and Ca oxide in excess over the ideal cuprate composition) and heat treatment, we found combinations of the superconducting ($y = 1$) Tl cuprates with n = 2, 3, and 4, a nonsuperconducting cubic Tl, Ba perovskite with cell parameter a = 4.28 Å, and small amounts of unreacted copper oxide. Each of the three superconducting cuprates has been obtained without admixture of any of the others in at least one sample, with only the cubic perovskite (and excess CuO) appearing as contaminants. An example is given in Fig. 1B that shows that XRD intensity plot for an ($n = 4$) sample. Although a given combination of composition and heat treatment gives reproducible results, the systematic study of the many compositional and thermal variables involved is not yet advanced sufficiently for a detailed correlation

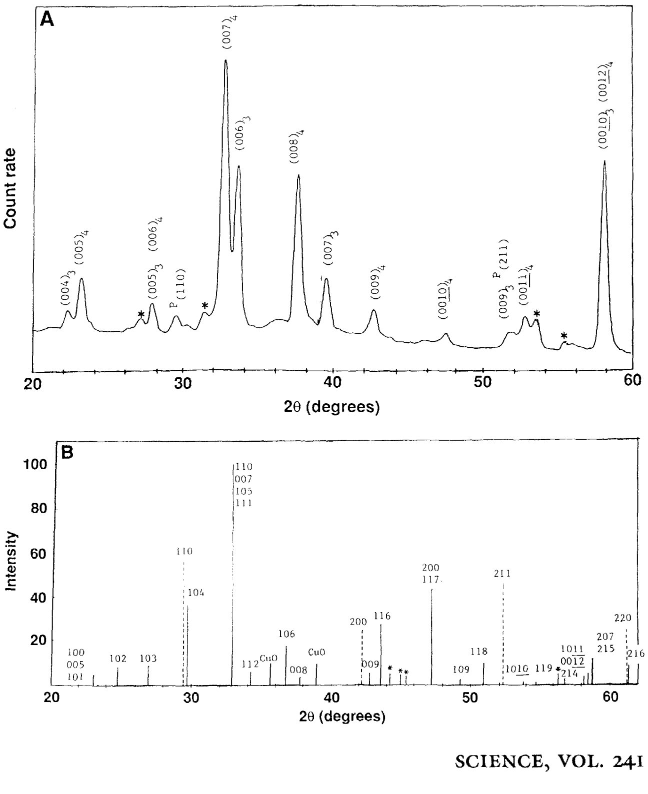

Fig. 1. (**A**) X-ray diffractogram (count rate in arbitrary units) for a sample of composition $Tl_{1.33}Pb_{0.5}Ba_2Ca_{3.33}Cu_4O$, aligned with H ⊥ [001] in a field of 15 T and mounted in epoxy, showing the {001} planes of ($n = 3$) and ($n = 4$) cuprate particles. There are small admixtures of perovskite and other, unidentified (probably also magnetically aligned) phases. (**B**) Indexed XRD intensity (in arbitrary units) for a sample of composition $Tl_{1.33}Ba_{1.33}Ca_4Cu_4O_x$ containing predominantly the ($n = 4$) phase $Tl(Ba_{0.5 0.5}Ca)_2Ca_3Cu_4O_z$, with admixtures of cubic Tl,Ba perovskite (dashed lines and small amounts each of excess CuO and an unidentified constituent (*).

P. Haldar, A. Roig-Janicki, B. C. Giessen, Department of Chemistry and Barnett Institute of Chemical Analysis and Materials Science, Northeastern University, Boston, MA 02115.
K. Chen, B. Maheswaran, N. K. Jaggi, Department of Physics, Northeastern University, Boston, MA 02115.
R. S. Markiewicz, Department of Physics and Barnett Institute of Chemical Analysis and Materials Science, Northeastern University, Boston, MA 02115.

*Present address: Department of Physics, Boston University, Boston MA 02215.

of these variables with the resulting phases.

The lattice parameters of the three cuprates are listed in Table 1; their primitive tetragonal unit cells (P4/mmm) with ideal atomic positions are shown in Fig. 2. Further crystallographic data will be published (*12*). The stacking sequence (with successive layers in $x = 0$, $y = 0$ and in $x = 1/2$, $y = 1/2$) is:

$$\cdots \mathrm{Tl} - \mathrm{Ba} - \mathrm{Cu} - [\mathrm{Ca} - \mathrm{Cu}]_{n-1} - \mathrm{Ba} \cdots \quad (1)$$

The *c*-axes for $n = 2$, 3, and 4 (Table 1) are consistent with the stacking sequence 1. For all *n*, the average distance between Cu planes is $d(\text{Cu-Cu}) \sim 3.1$Å. [Also included in Table 1 are data for the previously reported (Tl, Bi) single layer phases (*5, 6*) with $n = 1$ (*5*) and $n = 2$ (*6*), which contain Sr instead of Ba.]

Figure 3A shows the resistance measured on a mixed phase sample with 60% ($n = 4$) phase and 40% ($n = 3$) phase. This sample had $T_{c(\text{onset})} = 125$ K and $T_{c(R=0)} = 122$ K. This agrees closely with the onset of diamagnetism at 122 K measured on an oriented sample with >80% ($n = 4$) phase [mounted in epoxy (*9, 11*)] shown in Fig. 3B. T_c values are listed in Table 1.

Last, we discuss the observed variation of T_c with *n*. It has been proposed (*7*) that in the Bi cuprates only the $[\mathrm{CuO_2}]^{-2}$ layers contribute to the superconductivity, so that T_c should be a function of the volume fraction, f_s, of the material associated with these layers. To test this, we show in Fig. 4A the dependence of T_c on *n* for both the single and double Tl layer superconductors, expressed in a plot of log T_c versus $1/f_s$, where f_s is defined as follows. From Table 1, it can be seen that the following formula holds approximately for each cuprate:

$$c_n = c_{\mathrm{Tl}} + n c_{\mathrm{Cu}} \quad (2)$$

where c_n is the lattice parameter, $c_{\mathrm{Cu}} = 3.1$ Å is the average "thickness" of a single copper oxide layer (equal to the average distance between successive Cu planes, as seen in Fig. 2), and c_{Tl} is the net "thickness" of the Tl-oxide layer, taken as the distance between the centers of the Ba atoms sandwiching this layer. For a single Tl layer ($y = 1$), $c_{\mathrm{Tl}} \cong 6.5$ Å; for a double layer ($y = 2$), $c_{\mathrm{Tl}} \cong 8.5$ Å. Then

$$f_s = n c_{\mathrm{Cu}} / c_n \quad (3)$$

Various models (*7, 8*) have suggested

$$\ln T_c \sim \text{constant} - (f_s)^p \quad (4)$$

with $p = 1$ (*8*) or 2/3 (*7*). Figure 4A shows that the T_c data for the single Tl layer compounds are consistent with $p = 1$ up to and including $n = 4$ (however, $p = 2/3$ fits the data almost as well). Although the $y = 2$ points for Tl compounds fall on a common straight line, as shown in Fig. 4A, two different curves are required to fit the $y = 2$ data (*2, 3*) for Tl and Bi compounds, respectively.

One may try to integrate all of these data sets (Fig. 4B) by noting that for $y = 2$, the extra Tl layer has almost the same effect on T_c as an extra Cu layer, that is, $T_c(y = 2, n) \cong T_c(y = 1, n + 1)$. In fact, defining

$$f_s' = (n c_{\mathrm{Cu}} + c_{\mathrm{Tl}}')/(c_n/y) \quad (5)$$

with $c_{\mathrm{Tl}}' = 2.0$ Å for $y = 2$, brings the two curves from Fig. 4A into near coincidence (Fig. 4B). This c_{Tl}' is close to the crystallographic Tl layer thickness (the difference between a Ba-Tl-Tl-Ba and a Ba-Tl-Ba layer), $c_{\mathrm{Tl,cryst}} \approx 2.0$ Å. This result suggests

Table 1. Structure data and superconducting properties of single Tl,Bi layer phases of the series $(\mathrm{B^{III}})_1(\mathrm{A^{II}})_2\mathrm{Ca}_{n-1}\mathrm{Cu}_n\mathrm{O}_{2n+2.5+\delta}$.

Components	Short form	*a* (Å)	*c* (Å)	$T_{c(\text{onset})}$ (K)	$T_{c(R=0)}$ (K)	Ref.
$\mathrm{B^{III}} = \mathrm{Tl}$ $\mathrm{A^{II}} = (\mathrm{Ba,Ca})$	1212	3.847	12.74	98	90	This work
	1223	3.849	15.87	114	110	(*4*); this work
	1234	3.850	19.01	125	122	This work
$\mathrm{B^{III}} = (\mathrm{Tl,Bi})$ $\mathrm{A^{II}} = (\mathrm{Sr,Ca})$	1201 ("121")*	3.745	9.00	50	25	(*5*)
	1212	3.800	12.07	90	75	(*6*)

*Designation for the 1201 phase used in (*5*).

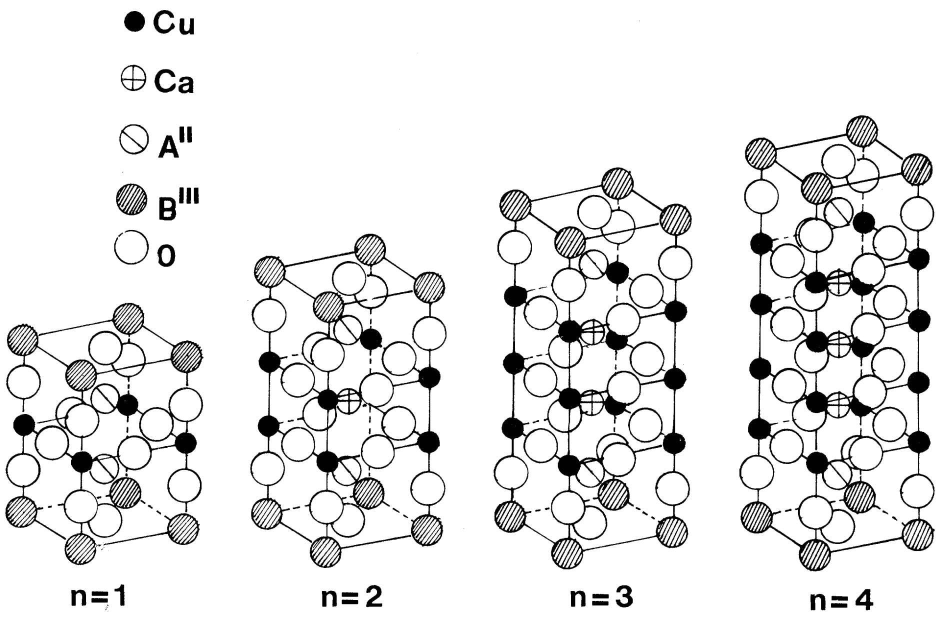

Fig. 2. Unit cells (with idealized atomic positions) of the first four members of the homologous series $\mathrm{Tl_1(A^{II})_2Ca}_{n-1}\mathrm{Cu}_n\mathrm{O}_z$, where $z = 2n + 2.5 + \delta$.

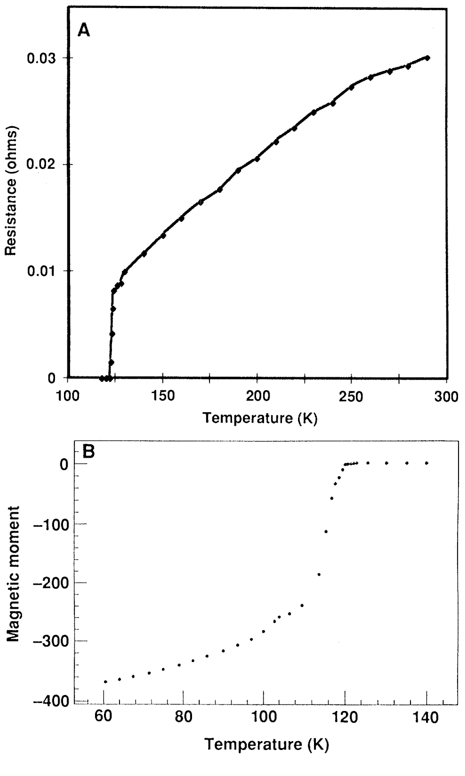

Fig. 3. (**A**) Resistance versus temperature for $(\mathrm{Tl_{0.5}Pb_{0.2}})_{1.25}(\mathrm{Ba_{0.5}Ca_{0.5}})_2\mathrm{Ca_3Cu_4O}_x$, which contains the $n = 4$ phase and the $n = 3$ phase. (**B**) Magnetic moment (arbitrary units) versus temperature for an aligned $\mathrm{Tl_{1.33}Ba_{1.33}Ca_4Cu_4O}_x$ sample that contains predominantly the $n = 4$ phase (see Fig. 1B).

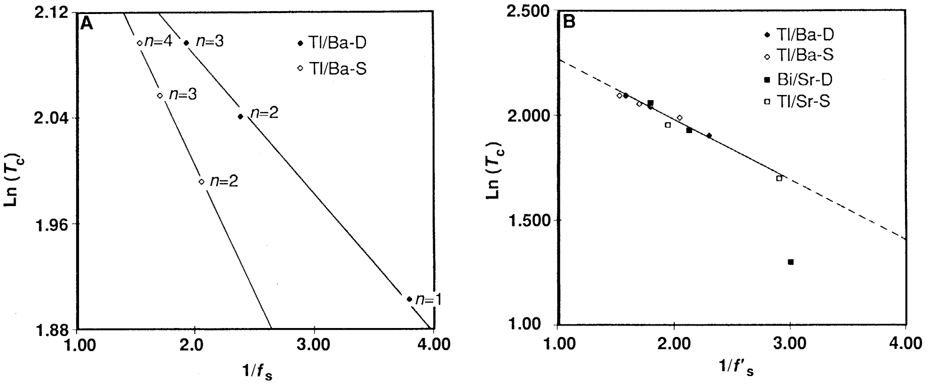

Fig. 4. (**A**) Plots of ln T_c versus $1/f_s$ for the two Tl(Ba) series with $y = 1$ and $y = 2$. (**B**) Master curve showing all four families scaled versus $1/f'_s$, where the "superconducting fraction" f_s is defined in Eq. 5. The symbols refer to different families: S, single B^{III} layer phase; D, double B^{III} layer phase.

that the Tl double layers play a contributing role in the superconductivity. On the other hand, the single Tl layers in a $y = 1$ phase and about 50% of the Tl double layer in a $y = 2$ phase formally do not contribute to T_c. We also include data for ($y = 1$) Tl compounds with Sr instead of Ba ($c'_{Tl} = 0$) and ($y = 2$) Bi compounds ($c'_{Bi} = 1.0$ Å). It can be seen that all data except the ($n = 1$) Bi compound fall on a common straight line that extrapolates to $T_c \approx 180$ K for the "pure" $f'_s = 1$ phase.

This extrapolation must be used with caution, since the Tl or Bi layer appears to be necessary for producing holes in the $[CuO_2]^{-2}$ layers. Thus the material with neither Tl nor Bi (or equivalent) layers is nonsuperconducting, and indeed semiconducting (*13*), even though formally $f_s = f'_s = 1$. Nevertheless, with an appropriate mix of Tl/Bi and Cu layers or by appropriate doping in the Ca^{2+} site, it may be possible to approach the extrapolated limit.

In conclusion, we have shown that T_c continues to increase with the number of Cu oxide layers for the single layer Tl cuprates at least to $n = 4$ and that the T_c data can be fitted to a common curve.

REFERENCES AND NOTES

1. C. C. Torardi *et al.*, *Science* **240**, 631 (1988).
2. M. A. Subramanian *et al.*, *Nature* **332**, 420 (1988).
3. S. S. P. Parkin *et al.*, *Phys. Rev. Lett.* **60**, 2539 (1988); *ibid.* **61**, 750 (1988).
4. R. M. Hazen, paper presented at the American Physical Society March Meeting, New Orleans, 21 to 25 March 1988; W. W. Maggs, *Eos* **69**, 236 (1988); R. Dagani, *Chem. Eng. News* **66**, 24 (16 May 1988).
5. P. Haldar, A. Roig-Janicki, S. Sridhar, B. C. Giessen, *Mater. Lett.*, in press.
6. P. Haldar *et al. J. Superconduct.* **1**, 211 (1988).
7. T. Schneider and D. Baeriswyl, in preparation.
8. P. Grant, paper presented at the Latin American Conference on High Temperature Superconductivity, Rio de Janeiro, May 1988.
9. D. E. Farrell *et al.*, *Phys. Rev. B* **36**, 4025 (1987).
10. R. H. Arendt *et al.*, in *High-Temperature Superconductivity*, M. B. Brodsky, R. C. Dynes, K. Kitazawa, H. L. Tuller, Eds. (Materials Research Society, Pittsburgh, PA, 1988), pp. 203–208.
11. K. Chen, B. Maheswaran, P. Haldar, R. S. Markiewicz, B. C. Giessen, in preparation.
12. A. Roig-Janicki, P. Haldar, B. C. Giessen, in preparation.
13. T. Siegrist, S. M. Zahurak, D. W. Murphy, R. S. Roth, *Nature* **334**, 231 (1988).

14. This work was supported by E. I. du Pont de Nemours & Company, Inc. Magnetic work was done at the Francis Bitter National Magnet Laboratory, which is supported at MIT by the National Science Foundation. N.K.J. acknowledges support by the Microelectronics and Computer Technology Corporation. We thank R. Peacetree for preparative work and J. Volf for secretarial assistance. This is publication 350 of the Barnett Institute.

22 July 1988; accepted 1 August 1988

Femtosecond Clocking of the Chemical Bond

MARK J. ROSKER, MARCOS DANTUS, AHMED H. ZEWAIL*

When a chemical bond is broken in a direct dissociation reaction, the process is so rapid that it has generally been considered instantaneous and thus unmeasurable. However, the bond does persist for times on the order of 10^{-13} seconds after the photon has been absorbed. Femtosecond (10^{-15} second) laser techniques can be used to directly clock this process, which describes the dynamics of the chemical bond. The time required to break the chemical bond in an elementary reaction has been measured and the characteristic repulsion length for the potential governing fragment separation has been obtained.

The structure of the chemical bond in molecules is now well characterized in a variety of systems. Until recently, however, the dynamics of the chemical bond have not been directly observed, because the relevant time scales involved are too rapid. For example, one might ask the question: how long does it take to break a chemical bond in the elementary reaction ABC + $h\nu \rightarrow$ A + BC? Two fundamental processes are involved in this reaction. The first, which is virtually instantaneous, is the transition of ABC from its ground (bound) potential energy surface (PES) to an excited (dissociative) PES. The second process, the so-called half-collision, involves the subsequent time evolution of the molecule on this dissociative PES. This evolution must lead to the spatial separation of the fragments; when the fragments no longer interact, the chemical bond is broken.

The terminal velocities of separation of the fragments for such reactions are typically ~1 km s^{-1} (=0.01 Å fs^{-1}). If the bond is considered to be broken when the fragments are a few times their equilibrium bond length apart (typically several angstroms), then the time required to break the bond must be of the order of a few hundred femtoseconds. Recent advances in ultrafast laser spectroscopy of chemical reactions (*1*–*5*) have allowed the observation of chemical bond dynamics on this time scale. We report the direct clocking measurement of bond-breaking time in the elementary reaction ICN + $h\nu \rightarrow$ I + CN.

The dissociation reaction of ICN on the repulsive surface passes through transition-state configurations,

$$\mathrm{ICN}^* \rightarrow [\mathrm{I}\cdots\mathrm{CN}]^{\ddagger *} \rightarrow \mathrm{I} + \mathrm{CN}$$

where the bond stretches from the initial value at R_0 to "infinite" separation, that is, when the I and CN fragments are sufficiently separated so as to no longer interact. Real-time observations of these transition states ($[\mathrm{I}\cdots\mathrm{CN}]^{\ddagger *}$) have been made with femtosecond transition-state spectroscopy (FTS), a technique for viewing the fragments en route to products (*2*). However, the absolute clocking of these transition states and of the final states (free fragments) was not established, since the exact zero-of-time was not determined. To measure the actual time for bond breaking and to obtain informa-

---

Arthur Amos Noyes Laboratory of Chemical Physics, California Institute of Technology, Pasadena, CA 91125.